

Doppler-free measurement of the 546 nm line of mercury

This article has been downloaded from IOPscience. Please scroll down to see the full text article.

2010 J. Phys. B: At. Mol. Opt. Phys. 43 205003

(<http://iopscience.iop.org/0953-4075/43/20/205003>)

View [the table of contents for this issue](#), or go to the [journal homepage](#) for more

Download details:

IP Address: 161.53.9.221

The article was downloaded on 08/10/2010 at 10:04

Please note that [terms and conditions apply](#).

Doppler-free measurement of the 546 nm line of mercury

Craig J Sansonetti and Damir Veza¹

National Institute of Standards and Technology, Gaithersburg, MD 20899, USA

E-mail: craig.sansonetti@nist.gov

Received 25 August 2010, in final form 26 August 2010

Published 5 October 2010

Online at stacks.iop.org/JPhysB/43/205003

Abstract

We have made Doppler-free observations of the 546 nm line of neutral mercury by using saturated absorption and frequency modulation spectroscopy. Absolute wave numbers were measured for 14 resolved components arising from six mercury isotopes. Combining these measurements with precisely known isotope shifts and hyperfine-structure splittings, we derive a value for the wave number in ^{198}Hg from each of the measured features. Our final value for the wave number of the ^{198}Hg line is in good agreement with a recently reported measurement using Fourier transform spectroscopy but has an uncertainty that is smaller by a factor of 12.

1. Introduction

The spectrum of neutral mercury has long been recognized as a particularly convenient source of calibration standards for interferometric wavelength measurements. Microwave-excited electrodeless-discharge lamps (EDLs) containing ^{198}Hg were developed especially for this purpose [1]. These lamps produce lines that are narrow, symmetric and highly reproducible. Nearly 50 years ago, Fabry–Perot interferometry was used to measure the mercury lines with respect to the ^{86}Kr primary standard in a number of precise experiments [2–5]. Wavelengths of four visible lines of ^{198}Hg based on these studies continue to be recommended by the International Committee for Weights and Measures (CIPM) as a practical realization of the meter with a relative expanded uncertainty (99% confidence) of 5×10^{-8} [6].

More recently Salit, Sansonetti, Veza, and Travis [7] used Fourier transform spectroscopy (FTS) to observe the spectrum of ^{198}Hg in the visible region as emitted by microwave-excited EDLs with argon buffer gas. The wavelengths of four strong lines and their shift rates as a function of buffer gas pressure were reported [7]. The measurements were made with respect to a tunable laser locked to a molecular iodine hyperfine component, which had in turn been measured with respect to an iodine-stabilized He-Ne laser [8]. As a consistency check, the measurements of [7] were repeated with the tunable laser locked to two different iodine lines. The work of Salit *et al* was extended to additional mercury lines, and the argon

pressure shift rates were determined with greater precision, by Veza *et al* [9]. The wavelength of the ^{198}Hg 546 nm line as determined in these FTS experiments was consistent with the CIPM recommendation within the 99% confidence interval of that recommendation. The FTS value differed from the CIPM recommendation, however, by 3.1 parts in 10^8 , considerably outside its own uncertainty of 1.8 parts in 10^8 at the 99% confidence level.

The internal consistency of the wave number scale in measurements made by high-resolution Fourier transform spectroscopy is often at the level of 1×10^{-8} or better. The absolute accuracy of the results, however, depends on a multiplicative correction of the scale based on internal standard lines. In recent observations of a hollow cathode lamp containing both iron and germanium, the wave number scales derived from lines of Fe I and from lines of Ge I were found to be inconsistent at the level of 6.5 parts in 10^8 [10]. The Ge I wavelengths used in determining the scale correction factor were measured by Fabry–Perot interferometry with respect to the 546 nm line of ^{198}Hg [11]. If the Ge I wavelengths used to calculate the scale correction were adjusted to reflect the revised mercury wavelength given by Salit *et al* [7], the discrepancy between the corrections based on Fe I and Ge I would be reduced.

In this work, we present new observations of the 546 nm line in natural mercury by Doppler-free laser spectroscopy. The line is complex, as mercury has seven stable isotopes, two of which have magnetic hyperfine structure. In our spectra 14 of the 16 underlying components were resolved. All resolved components were measured with an absolute accuracy of two

¹ Permanent address: Department of Physics, University of Zagreb, Zagreb, Croatia.

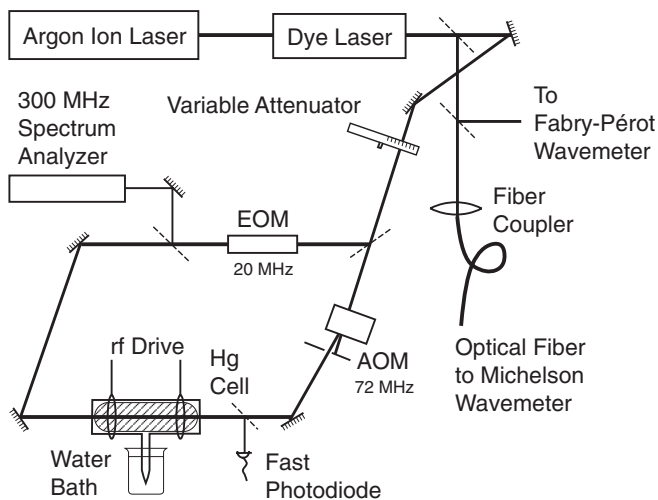


Figure 1. Apparatus diagram for observation of the mercury 546 nm line by Doppler-free saturated absorption or frequency modulation spectroscopy.

parts in 10^9 or better with respect to an iodine-stabilized He-Ne laser. Intervals among these components were previously reported with high precision by Rayman *et al* [12], Rayman [13] and McDermott and Lichten [14]. By combining their results with our absolute measurements, we can obtain an independent value for the ^{198}Hg line from each of the 14 measured components.

2. Experiment

The mercury spectrum was observed in a glass cell 10 cm long and 2.5 cm in diameter with a 7 mm diameter sidearm. The cell was outgassed and filled under vacuum with a few milligrams of mercury. Residual gas pressure at the time of filling was less than 2×10^{-5} Pa.

The 546 nm line is the transition between the $5d^{10}6s6p^3P_2$ and $5d^{10}6s7s^3S_1$ levels. In order to observe the line in absorption, we populated the metastable $5d^{10}6s6p^3P_2$ level by running a weak radio-frequency (rf) discharge in the mercury cell. The discharge was driven by a 74 MHz vacuum tube rf oscillator. Power was coupled to the discharge by a pair of loop antennae with a separation of 8 cm. In typical operating conditions for strong mercury components, the dc plate voltage of the oscillator was 70 V. For the weakest mercury components, we raised the voltage to as high as 270 V to increase the metastable population and improve the signal-to-noise ratio. The mercury vapour pressure in the cell was stabilized at 0.133 Pa (1.0 mTorr) by placing the sidearm in a beaker of water at a temperature of approximately 20° C. We were not able to obtain a stable discharge at lower mercury pressure.

The optical setup shown in figure 1 allowed us to obtain Doppler-free mercury spectra by either saturated absorption or frequency modulation (FM) spectroscopy. A commercial ring dye laser was operated with the dye Rhodamine 110 to produce tunable single-frequency radiation with a line width of less than 1 MHz. The laser beam was split into pump

and probe beams with an intensity ratio of about 2:1 that counterpropagated coaxially through the mercury discharge cell. The collimated beams were approximately 1.5 mm in diameter. The frequency of the pump beam was shifted upward by 72 MHz and its intensity was modulated sinusoidally at approximately 80 kHz by an acousto-optic modulator (AOM). The frequency shift introduced by the AOM isolates the dye laser from feedback due to the counterpropagating beams. Typical laser powers were 74 μW in the probe beam and 140 μW maximum in the modulated pump beam.

The probe beam was passed through a travelling wave electro-optic phase modulator (EOM). For FM spectroscopy this modulator created symmetric sidebands 20 MHz to either side of the laser centre frequency. The rf drive power to the EOM was adjusted to put 10% of the laser power in each sideband by observing the probe beam with a 300 MHz spectrum analyzer. The probe beam transmitted through the mercury cell was focused on a fast photodiode, and the resulting signal was amplified and processed by a double balanced mixer and lockin amplifier to recover the antisymmetric FM line profile. A complete description of our implementation of the FM method is given in [8]. The mercury resonances could be observed as Doppler-free Voigt profiles by simply turning off the drive to the EOM and connecting the photodiode signal directly to the lockin amplifier. This saturated absorption mode was used only to measure line widths and assess the symmetry of the line profiles.

All measurements were made by servo-locking the dye laser to the zero crossing of an FM resonance and determining the laser wave number with the Fabry-Pérot wavemeter developed in our laboratory [15]. This wavemeter has been used for a variety of precise measurements and has demonstrated a sub-MHz level of accuracy. Its measurements are made with respect to a He-Ne laser stabilized to the g component of the $^{127}\text{I}_2$ transition R(127)11-5. The laser was built to the same design as that used by Jennings *et al* [16], who determined the frequency of this line to be 473612340.492(74) MHz. Each measurement of a mercury component represents the average of about 12 successive readings from the wavemeter. The standard deviation of this average was typically $7 \times 10^{-6} \text{ cm}^{-1}$.

In order to correct for phase dispersion on reflection from the coatings of the Fabry-Pérot interferometer plates, as we have previously described [17], all lines were measured with both 218 mm and 11 mm interferometer spacers. The resulting phase correction calculated from these data alone was $-0.00394(16)$ order.

3. Results

The isotopic and hyperfine structure components of the 546 nm line are illustrated in figure 2. The odd mercury isotopes, ^{199}Hg and ^{201}Hg , have nuclear spins $I = 1/2$ and $3/2$, respectively. The nuclear spins couple to the angular momenta J of the fine structure levels to produce hyperfine sublevels with total angular momentum F . The hyperfine sublevels and their correspondence to the observed hyperfine components are shown in figure 3. We were able to measure 14 of the 16

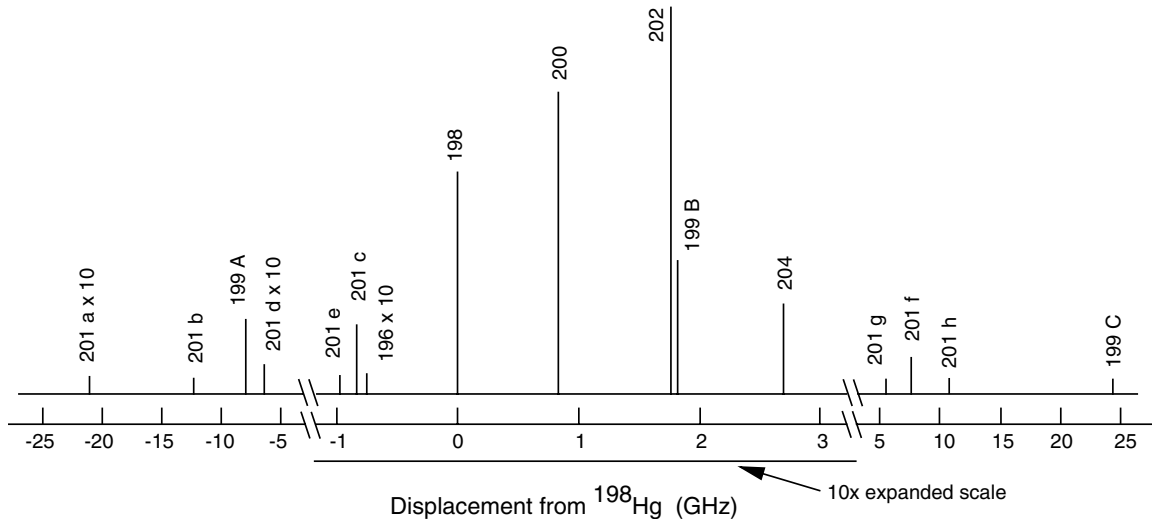


Figure 2. Isotopic and hyperfine structure of the mercury 546 nm line. Note that the frequency scale is expanded in the line centre and the intensity of the weakest components is multiplied by a factor of 10 for visibility.

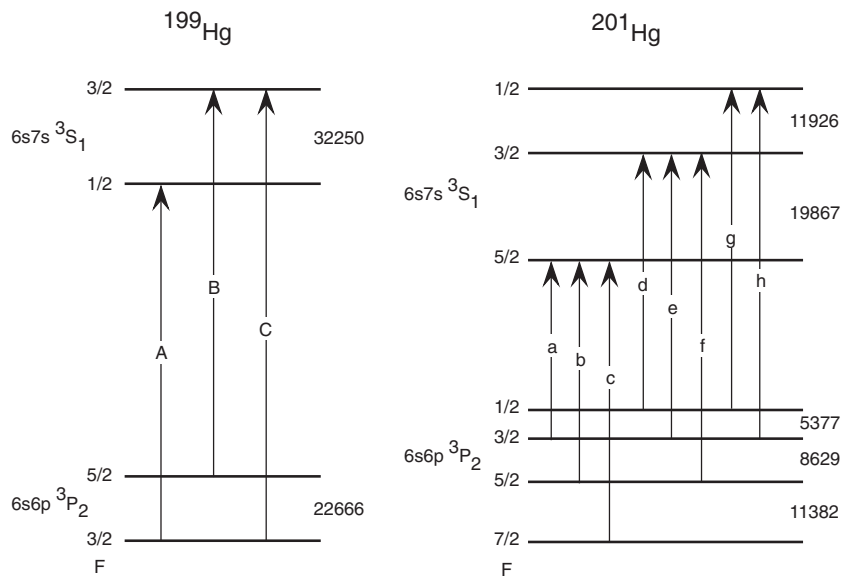


Figure 3. Energy level diagrams showing the hyperfine sublevels and transitions of the $6s6p\ ^3P_2$ and $6s7s\ ^3S_1$ levels of ^{199}Hg and ^{201}Hg . Intervals between the hyperfine sublevels are given in MHz.

components expected for the seven stable mercury isotopes. ^{196}Hg and ^{199}Hg component B could not be measured because they were perturbed by the much stronger adjacent lines of ^{201}Hg and ^{202}Hg . In order to measure the very weak ^{201}Hg components a and d, it was necessary to use increased rf power to the discharge and higher laser power. As a result, these components were noticeably broadened.

By taking differences of our measurements for various components, we can determine isotopic and hyperfine intervals that have been measured in previous experiments. In table 1 we compare our isotopic intervals for the even isotopes to the most precise literature values. In table 2 we present results for the intervals between hyperfine sublevels in the odd mercury isotopes. The uncertainties cited for our work in tables 1 and 2 include only statistical estimates of uncertainty. Systematic contributions from the uncertainty of the reference

Table 1. Isotopic structure intervals for even mercury isotopes in the 546 nm line. Uncertainties are reported at the one standard error level.

Interval	This work (MHz)	Literature (MHz)	Combined uncertainty (MHz)	Deviation (MHz)
$^{198}\text{Hg}-^{200}\text{Hg}$	846.25(32)	846.445(36) ^a	0.321	-0.19
$^{200}\text{Hg}-^{202}\text{Hg}$	930.83(27)	929.200(33) ^a	0.273	1.63
$^{202}\text{Hg}-^{204}\text{Hg}$	913.10(25)	914.327(51) ^a	0.259	-1.23
$^{200}\text{Hg}-^{204}\text{Hg}$	1843.93(32)	1843.527(61) ^a	0.329	0.40

^a Rayman *et al* [12].

laser frequency and the phase correction are common to all mercury components and cancel in determining the intervals.

Table 2. Hyperfine structure intervals in the odd isotopes of mercury. Uncertainties are reported at the one standard error level.

Isotope	Level	Interval	HFS components	This work (MHz)	Literature (MHz)	Combined uncertainty (MHz)	Deviation (MHz)
199	6s7s ³ S ₁	3/2–1/2	C–A	32 250.73(21)	32 250.111(718) ^a	0.749	0.62
201	6s7s ³ S ₁	5/2–3/2	e–a	19 867.37(29)			
			f–b	19 867.28(48)			
			Weighted average	19 867.34(25)	19 867.291(452) ^a	0.515	0.05
201	6s7s ³ S ₁	3/2–1/2	g–d	11 926.02(52)			
			h–e	11 926.49(44)			
			Weighted average	11 926.29(33)	11 926.476(331) ^a	0.470	–0.18
201	6s6p ³ P ₂	7/2–5/2	c–b	11 382.67(31)	11 382.6288(8) ^b	0.309	0.04
201	6s6p ³ P ₂	5/2–3/2	b–a	8630.24(34)			
			f–e	8630.16(44)			
			Weighted average	8630.21(27)	8629.5218(5) ^b	0.270	0.69
201	6s6p ³ P ₂	3/2–1/2	d–e	5377.32(34)			
			h–g	5377.79(59)			
			Weighted average	5377.44(29)	5377.4918(20) ^b	0.293	–0.05

^a Rayman *et al* [12].^b McDermott and Lichten [14].

In general the agreement with previous measurements is very good, but there are some discrepant values. Looking first at the even isotopes in table 1, the 198–200 and 200–204 intervals are in satisfactory agreement with the more accurate results of Rayman *et al* [12]. The 200–202 and 202–204 intervals, however, disagree with [12] by about five times the combined uncertainties. Although our measurement of the ²⁰²Hg line is very reproducible, it is almost certainly pulled to higher frequency by the partially resolved 199 B component which lies just 31.7 MHz away and has about one third its intensity. Typical line widths in our spectra were 41 MHz, approximately double the 19.4 MHz natural width of the transition. The observed width was probably limited by the discharge environment, as further reduction of the laser power produced no narrowing of the lines. Rayman *et al* [12] state that their observed width was 35 MHz.

We turn now to the odd isotopes in table 2. By reference to figure 3 it is apparent that some of the hyperfine intervals of ²⁰¹Hg can be determined from differences of more than one pair of components. These multiple values are shown in table 2 along with their weighted average. In every case, the multiple determinations agree within their uncertainties. Our results for the hyperfine intervals of the 6s7s ³S₁ level in both ¹⁹⁹Hg and ²⁰¹Hg are in good agreement with [12] and are more accurate for the larger intervals. The hyperfine intervals of the ²⁰¹Hg 6s6p ³P₂ level were measured with very high accuracy by McDermott and Lichten [14] by the atomic beam magnetic resonance method. Our results for the 7/2–5/2 and 3/2–1/2 intervals are in excellent agreement. For the 5/2–3/2 interval, our value is higher by 2.5 times the combined uncertainties. We cannot suggest an explanation for this discrepancy, as the two differences which determine the interval are in very good agreement and the components are well isolated in the spectrum.

Our measured wave numbers for all resolved components of the 546 nm line are presented in table 3. The result for each component is the average of six to eight independent

measurements made on different days. Two corrections were applied to the data to arrive at the values in table 3. First, the results were reduced by $1.5 \times 10^{-6} \text{ cm}^{-1}$ to correct for the actual iodine cell temperature [16] and intracavity power [18] of our iodine-stabilized reference laser. Second, a much larger correction was made to account for the phase change on reflection at the Fabry–Perot interferometer plates. Two methods were used to estimate this correction. As noted above, all resolved mercury components were measured with both 11 mm and 218 mm Fabry–Perot spacers. From these data, which are specific to the current experiment, we calculate a correction of 0.003 94(16) order. From previous work in our laboratory, we have accumulated phase correction data at about 150 points spanning the region 471 nm to 765 nm. These data can be fit very well by a second-degree polynomial, which produces an interpolated value at the 546 nm line of 0.003 38(9) order. Unfortunately, these values disagree by about three times their combined uncertainties. Because this systematic correction is large compared to the statistical uncertainty, we have averaged the two values and expanded the uncertainty to encompass the 95% confidence interval for both. The resulting correction is 0.003 66(45) order corresponding to a wave number correction of $83.9 \times 10^{-6} \text{ cm}^{-1}$.

In table 3 the first number given in parentheses is the statistical uncertainty of the reported value, defined as the standard error of the mean. This is the uncertainty used in combining results to obtain component intervals. The second number in parentheses is the total uncertainty given at the 95% confidence level. It was constructed by first combining in quadrature the statistical uncertainty, the $2.9 \times 10^{-6} \text{ cm}^{-1}$ uncertainty attributable to the reference laser wave number, and the $3.5 \times 10^{-6} \text{ cm}^{-1}$ uncertainty of the reference laser power and temperature correction. The result was doubled to provide a 95% confidence interval for these well-characterized contributions. This was in turn combined in quadrature with the $10.3 \times 10^{-6} \text{ cm}^{-1}$ uncertainty in the phase correction, estimated as described above, to produce the total uncertainty.

Table 3. Determination of ^{198}Hg wave number from all resolved components of the 546 nm line. The first number in parentheses after each entry represents the statistical uncertainty in the last digit of that entry at the one standard error level. A second number in parentheses represents the total uncertainty at the 95% confidence level.

Component	Measured wave number (cm^{-1})	Displacement ^a from ^{198}Hg (MHz)	^{198}Hg Wave number (cm^{-1})
201 a	18 306.709 718(7)(20)	−20 843.729(40)	18 307.404 990(7)
201 b	18 306.997 592(9)(23)	−12 214.207(40)	18 307.405 014(9)
199 A	18 307.145 627(6)(18)	−7776.212(721)	18 307.405 014(25)
201 d	18 307.193 054(9)(23)	−6354.282(67)	18 307.405 010(9)
201 e	18 307.372 422(7)(19)	−976.790(67)	18 307.405 005(7)
201 c	18 307.377 277(5)(17)	−831.578(40)	18 307.405 016(5)
198	18 307.405 008(7)(20)	0.000	18 307.405 008(7)
200	18 307.433 236(8)(21)	846.445(36)	18 307.405 001(8)
202	18 307.464 285(4)(16)	1775.645(49)	18 307.405 056(5)
204	18 307.494 743(7)(20)	2689.972(124)	18 307.405 015(8)
201 g	18 307.590 863(15)(32)	5572.194(331)	18 307.404 995(18)
201 f	18 307.660 293(13)(30)	7652.732(67)	18 307.405 026(13)
201 h	18 307.770 247(13)(39)	10 949.686(331)	18 307.405 005(17)
199 C	18 308.221 396(4)(16)	24 473.899(63)	18 307.405 034(5)
		Weighted Average	18 307.405 014(4)(16)

^a Derived from results of [12–14].

By combining intervals reported in [12, 14] and [13], we have derived the displacement of all other components of the 546 nm line from the ^{198}Hg component with sub-MHz accuracy. These results, which are shown in the third column of table 3, can be used to obtain an independent value for the ^{198}Hg wave number from every measured component. The results, given with their statistical uncertainties in the fourth column of table 3, are in good agreement with the exception of the value based on measurement of the ^{202}Hg line. The position of this line is almost certainly perturbed by the partially resolved 199 B component that lies at slightly higher frequency. We obtain a final value for the ^{198}Hg wave number by taking a weighted average of the results in table 3, excluding the ^{202}Hg value, where the weighting factors are taken to be the inverse squares of the statistical uncertainties. The total uncertainty of the average is determined as described above.

In table 4 we compare our new result for the ^{198}Hg wave number with values from the literature. Our result is adjusted by using the $-1.94(4) \times 10^{-6} \text{ cm}^{-1}/\text{Pa}$ argon shift rate determined in [9] to account for the argon buffer gas pressure in the mercury EDLs. The results of [7] and [9], determined by Fourier transform spectroscopy, are in excellent agreement with our current value. The FTS results derive their calibration from the iodine-stabilized He-Ne laser, as does our current value, but the way in which the mercury line is compared to the laser is entirely different. The other literature values were determined by using Fabry–Perot interferometry to measure the mercury line with respect to the 605.7 nm line of ^{86}Kr . The measurement of Terrien [5] agrees very well with our current result. The other Fabry–Perot measurements, however, produce systematically larger values for the wave number of the 546 nm line. The deviation is about 2.5 parts in 10^8 , far larger than the uncertainty of the krypton standard line, and is significant with respect to the measurement uncertainty. This does not appear to be due to the argon pressure correction

Table 4. Comparison our results with interferometric measurements of the 546 nm line made in ^{198}Hg electrodeless discharge lamps with argon buffer gas.

Argon pressure (Pa)	This work ^a (cm^{-1})	Literature (cm^{-1})	Deviation (cm^{-1})
33	18 307.404 950(16)	18 307.404 81(24) ^b	−0.000 14(24)
		18 307.4049(3) ^c	−0.0001(3)
		18 307.405 45(34) ^d	0.000 50(34)
		18 307.405 28(34) ^e	0.000 33(34)
		18 307.404 13(23) ^b	−0.000 11(23)
400	18 307.404 238(36)	18 307.4042(2) ^c	0.0000(2)
		18 307.404 78(34) ^d	0.000 54(34)
		18 307.404 85(13) ^f	0.000 61(14)
		18 307.404 88(7) ^f	0.000 64(8)
		18 307.404 25 ^g	−0.000 01

^a Result of this work adjusted for argon buffer gas pressure by using the argon shift rate from [9].

^b Salit *et al* [7].

^c Veza *et al* [9].

^d Kaufman [2].

^e Baird *et al* [3].

^f Bruce and Hill [4].

^g Terrien [5]. No estimate of uncertainty is given. Note that Terrien corrected his measured value to zero argon pressure and reported the corrected value in table III of [5]. We show here Terrien's uncorrected measurement for the 400 Pa lamp.

applied to our results, as the deviation for the 33 Pa lamps is about the same as for the 400 Pa lamps. We can offer no explanation for this discrepancy.

4. Conclusions

We have made precise observations of the 546 nm line of mercury by using Doppler-free laser spectroscopy. Fourteen

of the 16 isotopic and hyperfine components of the line were fully resolved and were measured with respect to an iodine-stabilized He-Ne laser with absolute accuracies ranging from 0.9 to 2.1 parts in 10^9 . Component intervals derived from these measurements are in good agreement with previously published data. For the hyperfine intervals of the $7s\ ^3S_1$ state of ^{199}Hg and ^{201}Hg , our current results are more accurate than previous data.

Based on our measurements of all resolved components and previously reported component intervals, we find the absolute wave number of the ^{198}Hg 546 nm line at 0 Pa argon pressure to be $18\,307.405\,014(16)\text{ cm}^{-1}$. The uncertainty of 8.7 parts in 10^{10} (95% confidence level) is an improvement over previous values by a factor of about 20. Our new value agrees well with recent measurements made using FTS, but differs systematically from most older results measured with respect to ^{86}Kr by Fabry–Perot interferometry. This may have a bearing on the recently reported discrepancy in the wave number scale of Fourier transform spectra calibrated with lines of Fe I versus spectra calibrated with lines of Ge I [10].

The 546 nm line emitted from a low pressure EDL containing ^{198}Hg and argon buffer gas remains a useful wavelength standard for high precision interferometry. The vacuum wave number for this line can be calculated with high precision for any desired argon pressure by adjusting the 0 Pa value reported here using the $-1.94 \times 10^{-6}\text{ cm}^{-1}/\text{Pa}$ argon shift rate determined in [9].

References

- [1] Meggers W F and Westfall F O 1950 *J. Res. Natl Bur. Stand.* **44** 447
- [2] Kaufman V 1962 *J. Opt. Soc. Am.* **52** 866
- [3] Baird K M, Smith D S and Hart K H 1963 *J. Opt. Soc. Am.* **53** 717
- [4] Bruce C F and Hill R M 1961 *Australian J. Phys.* **14** 64
- [5] Terrien J 1958 *Compt. Rend.* **246** 2362
- [6] Quinn T J 2003 *Metrologia* **40** 103
- [7] Salit M L, Sansonetti C J, Veza D and Travis J C 2004 *J. Opt. Soc. Am. B* **21** 1543
- [8] Sansonetti C J 1997 *J. Opt. Soc. Am. B* **14** 1913
- [9] Veza D, Salit M L, Sansonetti C J and Travis J C 2005 *J. Phys. B: At. Mol. Opt. Phys.* **38** 3739
- [10] Nave G and Sansonetti C J 2004 *J. Opt. Soc. Am. B* **21** 442
- [11] Kaufman V and Andrew K L 1962 *J. Opt. Soc. Am.* **52** 1223
- [12] Rayman M D, Aminoff C G and Hall J L 1989 *J. Opt. Soc. Am. B* **6** 539
- [13] Rayman M D 1985 Isotope shifts and hyperfine splittings in the $6^3P_2 - 7^3S_1$ transition of the stable Hg isotopes: an application of a new single laser scanning technique *PhD Dissertation* University of Colorado, Boulder, CO
- [14] McDermott M N and Lichten W L 1960 *Phys. Rev.* **119** 134
- [15] Sansonetti C J 1988 *Advances in Laser Science IV* ed J L Gole, D F Heller, M Lapp and W C Stwalley (New York: American Institute of Physics) p 548
- [16] Jennings D A, Pollock C R, Petersen F R, Drullinger R E, Evenson K M, Wells J S, Hall J L and Layer H P 1983 *Opt. Lett.* **8** 136
- [17] Gillaspay J D and Sansonetti C J 1991 *J. Opt. Soc. Am. B* **8** 2414
- [18] Layer H P, Rowley W R C and Marx B R 1981 *Opt. Lett.* **6** 188